

# Fracture Toughness Properties of Three Different Biomaterials Measured by Nanoindentation

Ji-yu Sun, Jin Tong

*Key Laboratory of Terrain-Machine Bionics Engineering (Ministry of Education, China),  
Jilin University (Nanling Campus), Changchun 130022, P. R. China*

---

## Abstract

The fracture toughness of hard biomaterials, such as nacre, bovine hoof wall and beetle cuticle, is associated with fibrous or lamellar structures that deflect or stop growing cracks. Their hardness and reduced modulus were measured by using a nanoindenter in this paper. Micro/nanoscale cracks were generated by nanoindentation using a Berkovich tip. Nanoindentation of nacre and bovine hoof wall resulted in pile-up around the indent. It was found that the fracture toughness ( $K_{IC}$ ) of bovine hoof wall is the maximum, the second is nacre, and the elytra cuticle of dung beetle is the least one.

**Keywords:** biomimetics, bionics, biomaterials, nanoindentation, laminated structure, fracture toughness

Copyright © 2007, Jilin University. Published by Science Press and Elsevier Limited. All rights reserved.

---

## 1 Introduction

Natural biomaterials have special structures and functions with well acclimatization through the evolution of exchanging material, energy and information with natural surroundings over millions of years. The biomaterial has long been a source of influence and inspiration for engineering design<sup>[1]</sup>. Some biomimetic methods now allow us to mimic the structure of biomaterials<sup>[2]</sup>.

Natural composite materials are renowned for their mechanical strength and toughness: despite being highly mineralized, with the organic component constituting only a few percent of the composite material, the fracture toughness exceeds that of single crystals of the pure mineral by two to three orders of magnitude<sup>[3]</sup>. The fracture toughness of hard materials is an important measure of the resistance of these materials to fracture and crack propagation<sup>[4]</sup>. The need for toughness arises because organisms are subjected to fluctuating forces and impacts during motion or through interaction with a moving environment<sup>[2]</sup>. Their structures would provide

some information for designing laminated structure material. There have been a number of efforts to make tough synthetic materials using layered structures<sup>[5]</sup>.

Recently, the structure and mechanical properties of shell were studied extensively<sup>[6–9]</sup>. While, it is difficult to measure their mechanical properties since the cuticle of bovine hoof wall and dung beetle are very thin. Nanoindenter gives a chance to resolve this problem. Motivated by this observation an overview is given in this paper on the understanding of the elastic behavior and the fracture toughness of nacre, bovine hoof wall and dung beetle (*Copris ochus* Motschulsky) cuticle.

Vincent and Wegst<sup>[10]</sup> demonstrated that since nearly all adult insects can fly, the cuticle has to provide a very efficient and lightweight skeleton. A most widely accepted comprehension is that insect cuticle is a composite consisting of chitin fibers and proteinaceous matrix in a layered structure<sup>[11,12]</sup>. On the basis of a microscopic study on bovine hoof wall, however, Wilkens suggested that the arrangement of tubule cortex cells more closely resembles the pattern of microsporophyll arrangement of pine cones although “pine cone” was

cells of the tubular cortex were organized generally into concentrically arranged lamellae, where each lamella was composed of one layer of cells<sup>[13]</sup>. Although lamellar thicknesses were generally constant, the tubule size was dependent on position in the wall.

## 2 Materials and methods

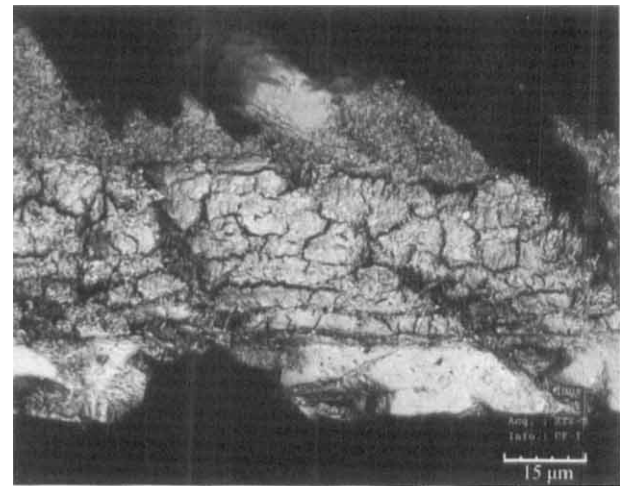
### 2.1 Specimens

Considering the laminated structure of those three different lamellar biomaterials, dung beetle cuticle, bovine hoof wall and nacre, the nanoindentation properties of cross section were investigated. The specimen preparation instrument (Phoenix Beta grinder/polisher, Buehler Ltd., USA) was used. After mounting in epoxy resin and polishing procedures, the cross section specimens of average RMS roughness ( $R_q$ ) 43.38 nm, 1.74 nm and 27.61 nm were prepared, respectively, which were smooth enough for nanoindentation test.

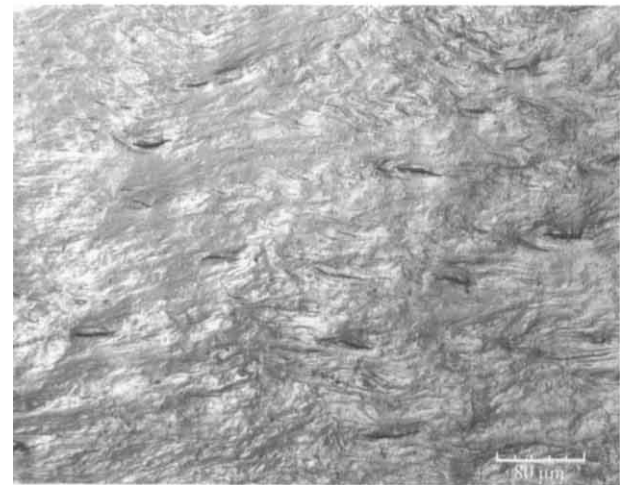
The confocal laser scanning microscope (LEXT OLS3000, Olympus Co., Ltd., Japan) was used to analyze the cross section morphology of dung beetle, bovine hoof wall and nacre.

Fig. 1a shows photograph of the cross section morphology of the elytra of dung beetle (*Coprins ochus* Motschulsky). Fig. 1b illustrates the surface morphology of polished section of bovine hoof wall. This is the middle layer of bovine hoof wall.

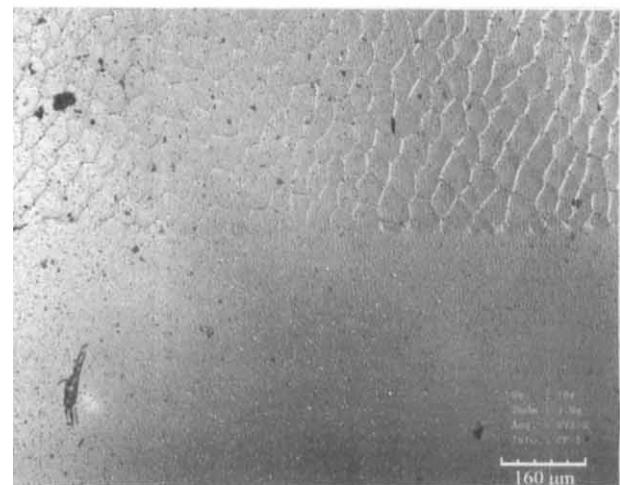
The shell was slanting put into cold mounting epoxy resin and then polished. Fig. 1c shows the optical microscopy photograph of the section of prismatic layer and nacreous layer (*Lamprotula fibrosa* Heude). Biological laminated material often exhibits intricate microstructures or micro-architectures. By using fiber like morphologies of the laminated phase and assembling the fibers into interpenetrating, as in elytra cuticle (Fig. 1a), or into cross-ply laminated structures, as in crossed lamellar mollusk shell (Fig. 1b), these materials obtain useful mechanical properties, including high hardness and fracture resistance. The spines of echinoderms (Fig. 1c) represent a remarkable case in which fully devise loading-bearing elements of the structure are separated by highly porous regions reminiscent of so-called “cellular materials”. Nevertheless, the entire structure is essentially a single crystal of calcite.



(a) Elytra cuticle of dung beetle



(b) Bovine hoof wall



(c) Nacre

**Fig. 1 Comparison of biological laminated structures (optical microscope photographs).**

## 2.2 Nanoindentation test

A nanoindenter (TriboIndenter, Hysitron Inc., USA) was used to investigate nanoindentation properties of those three biomaterials in this work. This instrument offers precision staging for automated testing and sample positioning. A Berkovich tip was used for the tests. The thermal drift effects were corrected for each test using a holding segment in the air before indentation. All nanoindentation tests were performed when the thermal drift was  $<0.05 \text{ nm}\cdot\text{s}^{-1}$ . The obtained load–displacement curves were automatically corrected for thermal drift by the system.

Based on Oliver-Pharr method<sup>[14]</sup> for determining the nanoindentation modulus and hardness, the initial unloading contact stiffness ( $S$ ) was obtained from slope of the unloading segment of force-displacement curve, as shown in Fig. 2. Then the hardness ( $H$ ) and reduced modulus ( $E_r$ ) were calculated<sup>[15,16]</sup>.

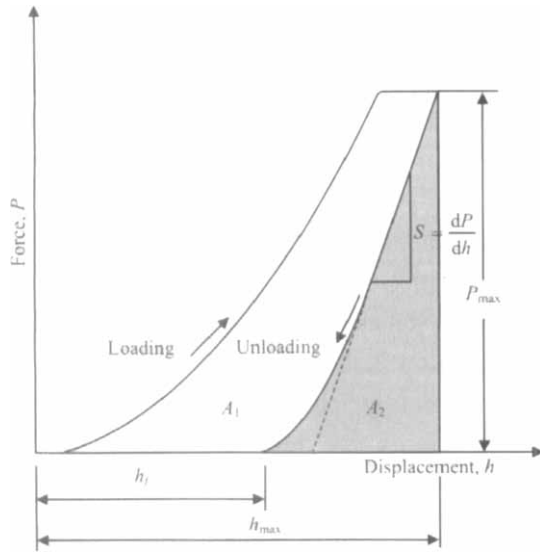


Fig. 2 The typical force-displacement curve by using nanoindenter which has three segments: loading, holding and unloading.  $A_1$  and  $A_2$  are the areas of plastic deform region and viscoelastic recover region, respectively.

The tip area function and machine compliance, were calibrated prior to each set of experiments using a fused quartz sample. The coefficients of contact area are iterative as:  $C_0 = 24.5$ ,  $C_1 = -7.7830 \times 10^3$ ,  $C_2 = 5.4605 \times 10^5$ ,  $C_3 = -4.4067 \times 10^6$ ,  $C_4 = 7.1034 \times 10^6$ ,  $C_5 = -3.3349 \times 10^6$ . For the present machine setup, the measured machine compliance is  $2.49 \text{ nm}\cdot(\text{mN})^{-1}$ .

To avoid the influence of the substrate materials on the measurements of the mechanical properties of specimen, the penetration depth should be less than 10 percent of the specimen thickness<sup>[17]</sup>. Thus, a maximum load of  $500 \mu\text{N}$  was used in this investigation to ensure that the indents were not too deep.

Considering biomaterials often exhibit viscoelastic deformation characteristics, the holding time and the loading rate during the indentation tests must be considered<sup>[18,19]</sup>. It was shown that the  $E_r$  and  $H$  values of cuticle of dung beetle were beyond 49% and 130% to the valid values, respectively, when the effect of viscoelastic deformation was ignored<sup>[20]</sup>. So a trapezoidal-type loading function was utilized for the indentation tests, the peak load was  $500 \mu\text{N}$ , the loading rate was  $53 \mu\text{N}\cdot\text{s}^{-1}$ , and the holding time was  $20 \text{ s}$ <sup>[21]</sup>. This limited the indent penetration depth to less than  $100 \text{ nm}$  or  $<10\%$  of the cuticle thickness. Ten repeating indentations were conducted to determine the average values of the  $E_r$  and  $H$ .

## 3 Results and discussion

The cross section specimens of nacre, elytra cuticle of dung beetle and bovine hoof wall are presented in successively decreasing values of the reduced modulus and hardness. The higher value the reduced modulus is the more stiffness the material has. The testing results are shown in Table 1. Viscosity of bovine hoof wall is the strongest, elytra cuticle of dung beetle and nacre is the following. The major possible reason is their different material composition. The bovine hoof wall is composed of keratin which has high retractility. The cuticle of dung beetle is composed of chitin fibre and protein matrix which give a firm and flexible combination. The nacre is combination of calcium carbonate crystal and organic matter matrix which has great toughness.

Table 1 The contrast of nanoindentation properties of three different lamellar biomaterials.

Specimens	$E_r$ (GPa)	$H$ (GPa)
Bovine hoof wall	$5.70 \pm 0.20$	$0.29 \pm 0.02$
Elytra cuticle of dung beetle	$6.17 \pm 0.15$	$0.33 \pm 0.01$
Nacre	$59.66 \pm 0.33$	$3.42 \pm 0.02$

When the sharp tip (such as Vicker tip or Berkovich tip) impresses on a brittleness material, the radial crack will be brought out. The relationship of impression and radial cracks is illustrated in Fig. 3<sup>[16]</sup>. The connection of fracture toughness ( $K_C$ ) and the length of the radial crack ( $c$ ) is deduced in theory expression of indent-crack mechanics<sup>[21]</sup>.

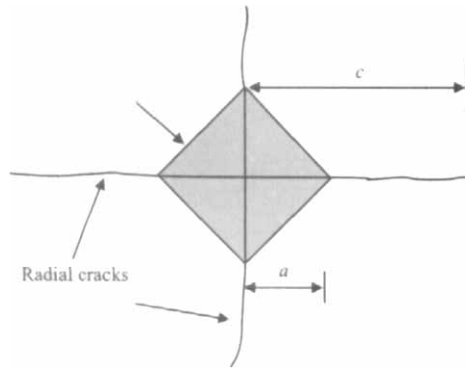


**Fig. 3 Schematic illustration of radial cracking at a Vickers indentation.**

$$K_C = \alpha \left( \frac{E_r}{H} \right)^{1/2} \left( \frac{P}{c^{3/2}} \right), \quad (1)$$

where  $\alpha$  is the empirical constant related to tip geometry. In-situ post-indentation images are obtained immediately after indentation. The lengths of the radial crack ( $c$ ) are measured directly from the images.

While  $\alpha$  has another deduced way<sup>[22]</sup>,

$$\alpha = \xi (c \cdot \tan \phi)^{2/3}, \quad (2)$$

where  $\xi$  is a constant decided by experiment system which is equal to  $0.032 \pm 0.002$  in a general way;  $\phi$  is half of angel of tip. For Vicker tip, Berkovich and Cube-corner tip,  $\phi$  is equal to  $68^\circ$ ,  $65.3^\circ$  and  $35.26^\circ$ ,  $\alpha$  is equal to 0.0175, 0.016 and 0.032<sup>[23–25]</sup>, respectively.

For more clearly morphological images, the maximum load used in experiment is 5000  $\mu\text{N}$ . Take  $E_r$ ,  $H$  and  $c$  into Eq. 1, the fracture toughness ( $K_C$ ) of three biomaterials in radial direction were obtained (shown in Table 2). It was found that the fracture toughness ( $K_C$ ) of bovine hoof wall is the maximum, the second is nacre, the elytra cuticle of dung beetle is the least one. Those indicate that the capability of resisting crack extending of cuticle of dung beetle is the worst. Biological strong material, like beetle cuticle, can resist outside force but appearance brittleness deformation easily<sup>[26]</sup>. The stronger fracture toughness of nacre is mainly the result

of cooperation of many kinds toughening mechanisms of crack defluxion and bridge graft of organic matrix<sup>[27]</sup>. Those mechanisms are associated with the so-called crossed lamellar micro-architecture of the shell, which provides for channel cracking in the outer layers and uncracked structural features that bridge crack surfaces, thereby significantly increasing the work of fracture of the material<sup>[3]</sup>.

**Table 2 Fracture toughness ( $K_C$ ,  $\text{MPa}\sqrt{\text{m}}$ ) of elytra cuticle of dung beetle, bovine hoof wall and nacre in radial direction which from up to down with clockwise.**

Specimen	$K_C$
Bovine hoof wall section	$8.71 \pm 2.59$
Elytra cuticle of dung beetle	$1.56 \pm 0.25$
Nacre section	$6.79 \pm 1.53$

Impress morphological images produced by nano-indentation test of section of bovine hoof wall, elytra cuticle of dung beetle and nacre are shown in Fig. 4, Fig. 5 and Fig. 6, respectively.

For lucubrate properties of materials, the appraised parameters of brittleness ( $B$ ) was brought forward<sup>[28]</sup>.

$$B = \frac{H}{K_C} \quad (3)$$

Table 3 illustrates the experimental results of brittleness properties of bovine hoof wall, elytra cuticle of dung beetle and nacre. It was found that their brittleness properties follow in descending order with elytra cuticle of dung beetle, nacre and bovine hoof wall. Those phenomena maybe are relatively with their various compositions. The mainly composition of nacre, cuticle of dung beetle and bovine hoof wall are aragonite, keratin and chitin embedded protein matrix, respectively. Aragonite is rigidity brittleness material. Keratin has higher stretch capability. Chitin has highness elastic, surrounded by protein matrix that it has lower brittleness in cuticle of dung beetle.

**Table 3 The comparison of brittleness ( $B$ ,  $1/\sqrt{\text{m}}$ ) of three kinds of biomaterials in radial directions.**

Specimen	$B$ (nm)
Bovine hoof wall section	$35.40 \pm 8.83$
Elytra cuticle of dung beetle	$216.82 \pm 39.67$
Nacre section	$527.57 \pm 106.44$

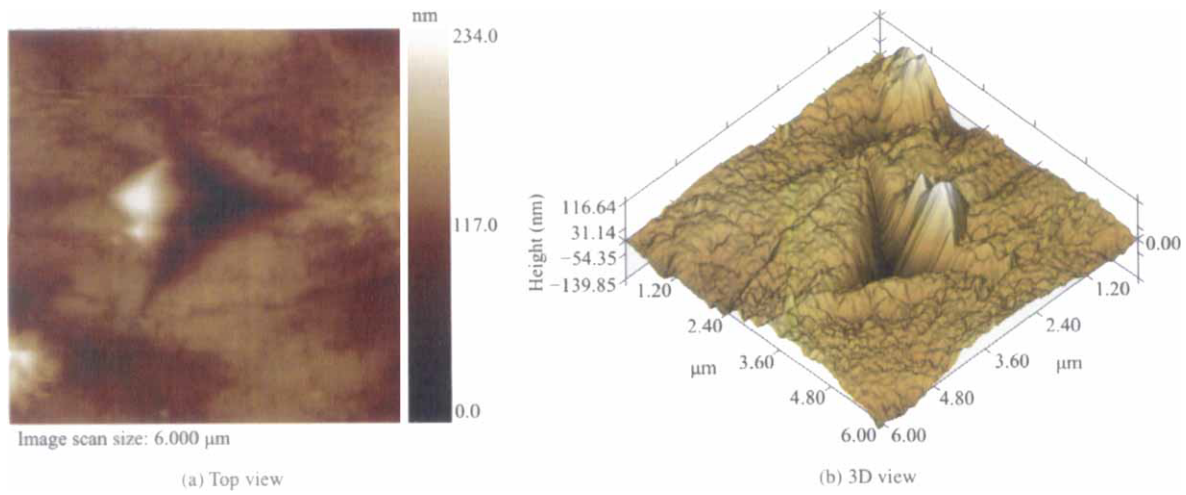


**Fig. 4 Impress morphological images produced by nanoindentation test of bovine hoof wall.**

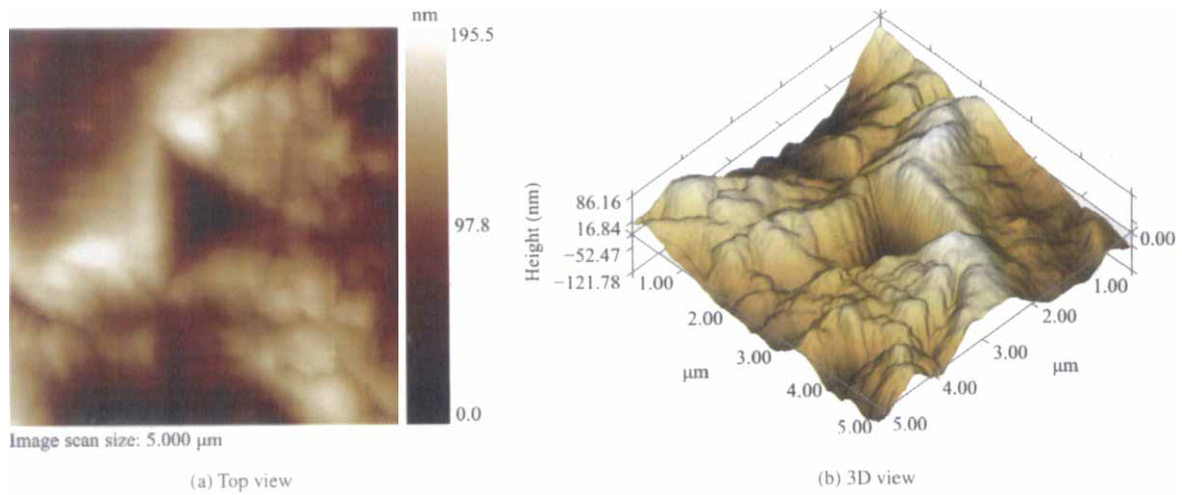


**Fig. 5 Impress morphological images produced by nanoindentation test of elytra cuticle of dung beetle.**

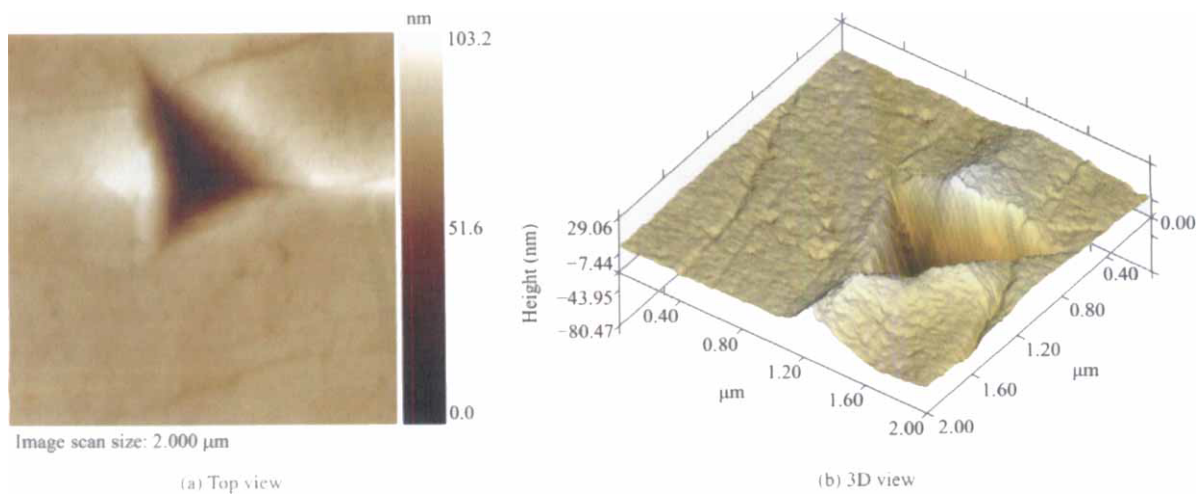


**Fig. 6 Impress morphological images produced by nanoindentation test of nacre.**

Calling  $\zeta$  the plastic index for investigating the plastic deform properties of material, shown in following<sup>[29]</sup>,

$$\zeta = \frac{A_1}{A_1 + A_2}, \quad (4)$$

where  $A_1$  and  $A_2$  are the areas of plastic deform region and viscoelastic recover region, respectively.

When  $A_2=0$ ,  $\zeta=1$ , it belongs to utterly plastic deform; when  $A_1=0$ ,  $\zeta=0$ , it belongs to utterly elastic deform; when  $0 < \zeta < 1$ , it belongs to viscoelastic-plastic deform.

Fitting the curves of loading, holding and unloading segments, the curve areas were acquired by integral, and then the plastic index was obtained.

In Table 4, it was found that the plastic index ( $\zeta$ ) of elytra cuticle of dung beetle was the least, supposed that its extent of plastic deformation was minimum and its visco-elastic recover was better. The  $\zeta$  values of nacre and bovine hoof wall were larger than dung beetle's, which were nearly 0.8 and assumed that have huge extent of plastic deformation.

**Table 4 The result of area of plastic deform region ( $A_1$ ), area of visco-elastic recover region ( $A_2$ ) and plastic index ( $\zeta$ ) of those biomaterials**

Specimen	$A_1$ (nm <sup>2</sup> )	$A_2$ (nm <sup>2</sup> )	$\zeta$
Nacre	643871.94	177299.65	0.78
Elytra cuticle of dung beetle	839830.17	456642.15	0.65
Bovine hoof wall	1875952.06	540479.67	0.78

It was found that surfaces of nacre and bovine hoof wall appearance pile-up phenomenons, supposed that those materials have intensive plastic deform which coincident with the  $\zeta$  value listed in Table 4. Learn from the impress morphological images, those three materials indicated the obviously anisotropy characters. It likely related with their anisotropic structure.

## 4 Conclusions

It was found that the fracture toughness ( $K_C$ ) of bovine hoof wall is the maximum, and the elytra cuticle of dung beetle is the least one. Their brittleness properties are also discussed which is following in descending order with elytra cuticle of dung beetle, nacre and bovine

hoof wall. The nanoindentation of nacre and bovine hoof wall results in pile-up around the indent. The  $\zeta$  values of nacre and bovine hoof wall are larger than dung beetle's, which are nearly 0.8 and assumed that they have larger plastic deformation properties.

## Acknowledgement

This work was supported by National Natural Science Foundation of China (grant no.30600131, 50675087), by National Science Fund for Distinguished Young Scholars of China (grant no. 50025516), by Special Research Fund for the Doctoral Program of High Education of China (grant no. 20060183067) and by "Project 985" of Jilin University.

## References

- [1] Sanchez C, Arribart H, Guille M, Madeleine G. Biomimetism and bioinspiration as tools for the design of innovative materials and systems. *Nature Materials*, 2005, **4**, 277–288.
- [2] Mehmet S. An introduction to biomimetics: A structural viewpoint. *Microscopy Research and Technique*, 2005, **27**, 360–375.
- [3] Kamat S, Su X, Ballarini R, Heuer A H. Structural basis for the fracture toughness of the shell of the conch *Strombus gigas*. *Nature*, 2000, **405**, 1036–1040.
- [4] Ji B H, Gao H J. Mechanical properties of nanostructure of biological materials. *Journal of the Mechanics and Physics of Solids*, 2004, **52**, 1963–1990.
- [5] Calvert P, Cesarano J, Chandra H, Denham H, Kasichainula S, Vaidyanathan R. Toughness in synthetic and biological multilayered systems. *Philosophical Transactions of the Royal Society A: Mathematical, Physical and Engineering Sciences*, 2002, **360**, 199–209.
- [6] Menig R, Meyers M H, Meyers M A, Vecchio K S. Quasi-static and dynamic mechanical response of *Haliotis rufescens* (abalone) shells. *Acta Materialia*, 2000, **48**, 2383–2398.
- [7] Maiera P, Richterb A, Faulkner R G, Riesb R. Application of nanoindentation technique for structural characterisation of weld materials. *Materials Characterization*, 2002, **48**, 329–339.
- [8] Li X D, Nardi P. Micro/nanomechanical characterization of a natural nanocomposite material — The shell of *Pectinidae*. *Nanotechnology*, 2004, **15**, 211–217.
- [9] Katti K, Katti D R, Tang J, Pradhan S, Sarikaya M. Modeling

- mechanical responses in a laminated biocomposite: Part II Nonlinear responses and nuances of nanostructure. *Journal of Materials Science*, 2005, **40**, 1749–1755.
- [10] Vincent J F V, Wegst U G K. Design and mechanical properties of insect cuticle. *Arthropod Structure & Development*, 2004, **33**, 187–199.
- [11] Scherge M, Gorb S S. *Biological Micro- and Nanotribology: Nature's Solutions*, Springer-Verlag, Berlin, Germany, 2002, 131–132.
- [12] Vincent J F V. Arthropod cuticle: A natural composite shell system. *Composites: Part A: Applied Science and Manufacturing*, 2003, **33**, 1311–1315.
- [13] Mario A K, John M G. Design complexity and fracture control in the equine hoof wall. *Journal of Experimental Biology*, 1997, **200**, 1639–1659.
- [14] Oliver W C, Pharr G M. Measurement of hardness and reduced modulus by instrumented indentation: Advances in understanding and refinements to methodology. *Journal of Material Research*, 2004, **19**, 3–20.
- [15] Vanlandingham M R. Review of instrumented indentation. *Journal of Research of the National Institute of Standards and Technology*, 2003, **108**, 249–265.
- [16] Hay J L, Pharr G M. Instrumented Indentation Testing. In: *ASM Handbook, Vol 8: Material Testing and Evaluation*, 10th edition, Kuhn H, Medlin D (ed), International Materials Park, Ohio, USA, 2000, 232–242.
- [17] Fischer-Cripps A C. *Introduction to Contact Mechanics*, Springer-Verlag, New York, USA, 2000, 14.
- [18] Ngan A H W, Tang B. Viscoelastic effects during unloading in depth-sensing indentation. *Journal of Materials Research*, 2002, **17**, 2604–2610.
- [19] Miyajima T, Nagata F, Kanematsu W, Yokogawa Y, Sakai M. Elastic/plastic surface deformation of porous composites subjected to spherical nanoindentation. *Key Engineering Materials*, 2003, **240–242**: 927–930.
- [20] Tong J, Sun J Y, Chen D H, Zhang S J. Factors impacting nanoindentation testing results of the cuticle of dung beetle *Copris ochus* Motschulsky. *Journal of Bionics Engineering*, 2004, **1**, 221–230.
- [21] Harding D S, Oliver W C, Pharr G M. Cracking during nanoindentation and its use in the measurement of fracture toughness. In: *Thin Films-Stresses and Mechanical Properties V, MRS Symposium Proceeding*, Baker S P (ed), 1995, **356**, 663–668.
- [22] Lawn B R, Evans A G, Marshall D B. Elastic/plastic indentation damage in ceramics: The median/radial crack system. *Journal of the American Ceramic Society*, 1980, **63**, 574–581.
- [23] Ostojic P, McPherson R. Review of indentation fracture theory: Its development, principles and limitations. *International Journal of Fracture*, 1987, **33**, 297–312.
- [24] Jackson A P, Vincent J F V, Turner R M. The mechanical design of nacre. *Proceedings of the Royal Society of London. Series B, Biological Sciences*, 1988, **234**, 415–440.
- [25] Anstis G R, Chantikul P, Lawn B R, Marshall D B. A Critical evaluation of indentation techniques for measuring fracture toughness: I, Direct Crack Measurements. *Journal of American Ceramic Society*, 1981, **64**, 533–538.
- [26] Ma H Z. *Introduction of Biological Mechanism*, College of Beijing Aviation Press, Beijing, China, 1986, in Chinese.
- [27] Sarikaya M, Liu J, Aksay L A. *Biomimetics: Design and Processing of Materials*, American Institute of Physics, New York, USA, 1995, 34–90.
- [28] Lawn B R, Marshall D B. Hardness, toughness, and brittleness: An indentation analysis. *Journal of American Ceramic Society*, 1979, **62**, 347–350.
- [29] Giannakopoulos A E, Suresh S. Determination of elastoplastic properties by instrumented sharp indentation. *Scripta Materialia*, 1999, **40**, 1191–1198.